Applicability of the Dirac–Fock method combined with core polarization for calculating atomic properties of alkali-metal atoms

Bobylev A. A.[1,2], Solovyev D. A.[1,2], Zalialiutdinov T. A.[1,2]

[1]Petersburg Nuclear Physics Institute named by B.P. Konstantinov of National Research Centre «Kurchatov Institute», Gatchina, Russia

[2]St. Petersburg State University, St. Petersburg, Russia

Introduction

Calculations of atomic properties, such as polarizabilities, Stark shifts, and QED corrections, are of great interest for various theoretical and experimental applications:

- Precision spectroscopy
- Atomic clocks
- Metrology

(B. K. Sahoo, *Relativistic Calculations of Atomic Clock*, Springer (2016); C. Cheung et al., *Phys. Rev. Lett.* **124**, 163001 (2020); M. G. Kozlov et al., *Rev. Mod. Phys.* **90**, 045005 (2018))

In this work, we use the Dirac–Fock method combined with core polarization (DFCP). We present our variant of this approach, based on a local version of the Dirac–Hartree–Fock potential (LDFCP).

Advantage: the LDFCP method is simple to implement and does not require large computational resources.
Goal: to test the applicability of LDFCP for polarizabilities, blackbody-radiation (BBR) Stark shifts and the Bethe logarithm of alkali-metal atoms.

The LDFCP Method

Tang Yong-Bo et al., Chinese Phys. B **23**, 063101 (2014); V. A. Yerokhin et al., Phys. Rev. A **94**, 032503 (2016)

Effective single-electron approximation. The valence electron is considered in the self-consistent field of a frozen core. The correlation interaction between the core electrons and the valence electron is taken into account using a semiempirical core polarization (CP) potential.

The stationary Dirac equation for a central field $V(r)$ ($\hbar = c = 1$):

$$(-i\boldsymbol{\alpha} \cdot \nabla + \beta m + V(r))\psi_n(\mathbf{r}) = \varepsilon_n \psi_n(\mathbf{r}). \tag{1}$$

The wave function has the form

$$\psi(\mathbf{r}) = \frac{1}{r} \begin{pmatrix} g(r)\, \Omega_{\kappa m}(\mathbf{n}) \\ i f(r)\, \Omega_{-\kappa m}(\mathbf{n}) \end{pmatrix}, \tag{2}$$

where $\kappa = l(l+1) - j(j+1) - \frac{1}{4}$ is the relativistic angular quantum number.

The large $g(r)$ and small $f(r)$ components of the wave function are expanded in a finite basis set constructed using B-splines (W. R. Johnson et al., Phys. Rev. A **37**, 307 (1988)), subject to the dual kinetic balance (DKB) conditions (V. M. Shabaev et al., Phys. Rev. Lett. **93**, 130405 (2004)).

The LDFCP Method

Potential:

$$V(r) = V_{\mathrm{LDF}}(r) + V_{\mathrm{CP}}(r)\,, \tag{3}$$

- V_{LDF} — a local version of the Dirac–Hartree–Fock potential[1].
- V_{CP} — semiempirical core polarization potential:

$$V_{\mathrm{CP}}(r) = -\frac{\alpha_c}{2\,r^4}\left(1 - e^{-r^6/\rho_\kappa^6}\right), \tag{4}$$

α_c — static dipole polarizability of the core[2], ρ_κ — radial cutoff parameter, which is chosen empirically (depends on l and j).
The potential V_{CP} introduces a correction to the electric dipole transition operator:

$$r \longrightarrow r\left(1 - \frac{\alpha_c}{r^3}\left(1 - e^{-r^6/\rho_\kappa^6}\right)^{1/2}\right). \tag{5}$$

[1] V. M. Shabaev et al. 2005 Phys. Rev. A 72, 062105
[2] J. Mitroy et al 2010 J. Phys. B: At. Mol. Opt. Phys. 43 202001

Static Dipole Polarizability

The polarizability of an atom can be regarded as a measure of the response of the electron cloud to an external electric field.
The atomic polarizability can be represented as the sum of a scalar and a tensor part:

$$\alpha = \alpha_0 + \alpha_2 \frac{3m_a^2 - j_a(j_a+1)}{j_a(2j_a-1)}. \tag{6}$$

Scalar polarizability:

$$\alpha_0 = \frac{2}{3(2j_a+1)} \sum_n \frac{|\langle a\|\mathbf{d}\|n\rangle|^2}{E_n - E_a} \tag{7}$$

Tensor polarizability:

$$\alpha_2 = 4\left(\frac{5j_a(2j_a-1)}{6(j_a+1)(2j_a+1)(2j_a+3)}\right)^{1/2} \sum_n (-1)^{j_a+j_n} \begin{Bmatrix} j_a & 1 & j_n \\ 1 & j_a & 2 \end{Bmatrix} \times \frac{|\langle a\|\mathbf{d}\|n\rangle|^2}{E_n - E_a} \tag{8}$$

Here $\langle a\|\mathbf{d}\|n\rangle$ are reduced dipole matrix elements, the sums run over the complete spectrum (including the continuum); $\alpha_2 = 0$ for $j_a = 1/2$.

Results: scalar polarizability α_0

Table 1: Values of the static electric dipole scalar polarizability, α_0, in a.u. The data from Kiruga et al. (2026) are highlighted in blue.

n	n^2S	$n^2P_{1/2}$	$n^2P_{3/2}$	$n^2D_{3/2}$	$n^2D_{5/2}$
			Li		
2	163.8	126.8	126.8		
	164	126.89	126.91		
3	4128.4	27467	27471	-14456	-14458
	4130.2	28239	28237	-14916	-14914
			Na		
3	161.7	360.5	362.2	6438.4	6413.9
	162.44	359.94	361.63	6419.7	6395.3
4	3079.7	-4520.1	-4450.0	634577	633699
	3100.3	-4493.6	-4423.5	635610	634840
			K		
3				1429	1415
				1422	1408
4	286.9	607.8	618.5	35897	35703
	290.25	602.1	612.7	35990	35810

n	n^2S	$n^2P_{1/2}$	$n^2P_{3/2}$	$n^2D_{3/2}$	$n^2D_{5/2}$
			Rb		
4				586	553
				587	553
5	314.7	807.7	869.2	17806	17422
	318.28	805.0	868.0	18120	17740
			Cs		
5				-327	-423
				-328	-433
6	396.7	1307	1606	-7030	-9837
	399.57	1343	1655	-5620	-8330
			Fr		
6				-249	-584
				-259	-613
7	316.1	1174	2178	-1979	-9224
	316.3	1177	2213	-250	-7420

A. Kiruga et al, Computer Physics Communications 319, 109951 (2026)

Results: tensor polarizability α_2

Table 2: Values of the tensor electric dipole polarizability, α_2, in a.u. The data from Kiruga et al. (2026) are highlighted in blue.

n	$n^2P_{3/2}$	$n^2D_{3/2}$	$n^2D_{5/2}$
	Li		
2	1.53		
	1.61		
3	-2087	11078	15828
	-2167	11400	16283
	Na		
3	-89.25	-3587	-5090
	-88.38	-3574.6	-5071.8
4	-174.8	-149169	-212575
	-167.7	-149260	-212740
	K		
3		-487.0	-678.0
		-484.0	-674.0
4	-111.7	-7775	-10908
	-108.7	-7810	-10960
	Rb		
4		-58.0	-35.0
		-59.0	-35.0
5	-169.1	-1205	-1086
	-166.6	-1310	-1240
	Cs		
5		346.0	649.0
		356.0	675.0
6	-260.0	9364	18425
	-262.0	8736	17290
	Fr		
6		235.0	863
		233.0	890
7	-454.0	4546	19882
	-453.9	4032	18480

A. Kiruga et al, Computer Physics Communications 319, 109951 (2026)

Results: Rydberg states

Table 3: Values of the static electric dipole scalar polarizability for Rydberg states, in a.u. The data from Yerokhin et al. (2016) are highlighted in blue. The number in square brackets denotes the power of ten, $\times 10^{[\cdot]}$.

n	n^2S	$n^2P_{1/2}$	$n^2P_{3/2}$	$n^2D_{3/2}$	$n^2D_{5/2}$
			Rb		
15	0.317[8]	0.116[9]	0.127[9]	0.796[8]	0.740[8]
	0.317[8]	0.116[9]	0.127[9]	0.796[8]	0.740[8]
20	0.285[9]	0.120[10]	0.131[10]	0.567[9]	0.516[9]
	0.289[9]	0.118[10]	0.130[10]	0.631[9]	0.582[9]
30	0.554[10]	0.275[11]	0.303[11]	0.087[11]	0.772[10]
	0.554[10]	0.269[11]	0.297[11]	0.101[11]	0.905[10]
			Cs		
15	0.203[8]	0.245[9]	0.325[9]	−0.239[9]	−0.293[9]
	0.211[8]	0.210[9]	0.275[9]	−0.188[9]	−0.231[9]
20	0.214[9]	0.316[10]	0.421[10]	−0.270[10]	−0.329[10]
	0.226[9]	0.267[10]	0.350[10]	−0.212[10]	−0.258[10]
30	0.476[10]	0.883[11]	1.18[11]	−0.671[11]	−0.813[11]
	0.511[10]	0.740[11]	0.972[11]	−0.526[11]	−0.636[11]

V. A. Yerokhin et al 2016 Phys. Rev. A 94, 032503

Dynamic Stark Effect Induced by Blackbody Radiation (BBR)

J. W. Farley, W. H. Wing, Phys. Rev. A **23**, 2397 (1981)

The electric field strength of blackbody radiation is determined through the blackbody radiation intensity (in relativistic units, $\hbar = c = 1$):

$$\mathcal{E}^2(\omega) = \mathcal{B}^2(\omega) = \frac{8}{\pi} \frac{\omega^3}{e^{\beta\omega} - 1}, \tag{9}$$

The effect of this field on an atom leads to a shift of the atomic energy level (dynamic Stark effect):

$$\begin{aligned} \Delta E_a^{\mathrm{BBR}} = & \frac{2}{3\pi\,(2j_a+1)} \sum_n \mathrm{P.V.} \int_0^\infty d\omega\, n_\beta(\omega)\, \omega^3 \\ & \times |\langle a \| \boldsymbol{d} \| n \rangle|^2 \left[\frac{1}{E_a - E_n + \omega} + \frac{1}{E_a - E_n - \omega} \right] \end{aligned} \tag{10}$$

where $n_\beta(\omega) = 1/[\exp(\beta\omega) - 1]$ is the Planck distribution, $\beta = 1/k_{\mathrm{B}}T$ (k_{B} is the Boltzmann constant, T is the temperature), ω is the frequency of the thermal photon, P.V. denotes the principal value of the integral.

M. A. Reiter et al., Phys. Rev. A **113**, 032801 (2026)

Results: BBR shifts

Table 4: Values of the thermal (BBR) Stark shift at a temperature of 300 K, in Hz. The values from Farley and Wing (1981) are highlighted in blue.

n	n^2S	$n^2P_{1/2}$	$n^2P_{3/2}$	$n^2D_{3/2}$	$n^2D_{5/2}$
			Li		
2	-1.41	-1.093	-1.094		
	-1.43	-1.145			
3	-38.1	46.56	46.57	-45.66	-45.64
	-38.62	50.80		-47.75	
			Na		
3	-1.388	-3.118	-3.133	-61.93	-61.95
	-1.389	-2.985	-2.998	-61.24	-61.25
4	-27.75	46.32	46.15	14.48	13.20
	-27.57	44.13	43.94	15.73	14.46
			K		
3				-13.03	-12.88
				-16.47	-16.30
4	-2.435	-5.251	-5.345	-160.5	-159.5
	-2.528	-5.370	-5.471	-171.9	-170.8

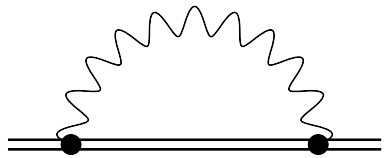
n	n^2S	$n^2P_{1/2}$	$n^2P_{3/2}$	$n^2D_{3/2}$	$n^2D_{5/2}$
			Rb		
4				-5.088	-4.787
				-6.467	-6.975
5	-2.645	-7.004	-7.553	-166.5	-160.1
	-2.789	-7.511	-8.127	-188.7	-181.4
			Cs		
5				3.517	4.649
				5.497	5.315
6	-3.300	-11.98	-15.24	-65.64	-102.0
	-3.589	-14.85	-17.24	-70.41	-99.18
			Fr		
6				2.89	6.84
7	-2.558	-10.43	-21.51	-60.98	-144.3

J. W. Farley, W. H. Wing, Phys. Rev. A 23, 2397 (1981)

Bethe Logarithm

H. A. Bethe, E. E. Salpeter (Springer, 1977); L. N. Labzowsky (Nauka, 1996)

Self-energy correction (Lamb shift), one-loop diagram:



In the lowest order for a hydrogen-like atom in an s state (atomic units), the one-loop self-energy correction is

$$\Delta E_a^{\mathrm{SE}} = \frac{4Z}{3}\alpha^3 \left(\frac{19}{30} - 2\ln \alpha Z - \ln k_0 \right) |\Psi(0)|^2 , \tag{11}$$

where $\ln k_0$ is the Bethe logarithm.
In the length gauge:

$$\ln k_0 = \frac{\sum\limits_n |\langle a|\mathbf{d}|n\rangle|^2 (E_n - E_a)^3 \ln |E_n - E_a|}{\sum\limits_n |\langle a|\mathbf{d}|n\rangle|^2 (E_n - E_a)^3}, \tag{12}$$

in the velocity gauge:

$$\ln k_0 = \frac{\sum\limits_n |\langle a|\mathbf{p}|n\rangle|^2 (E_n - E_a) \ln |E_n - E_a|}{\sum\limits_n |\langle a|\mathbf{p}|n\rangle|^2 (E_n - E_a)}. \tag{13}$$

Table 5: Bethe logarithm for ground states of Be^+ and alkali-metal atoms

Li (2s)	**Be**$^+$ (2s)	**Na** (3s)	**K** (4s)	**Rb (5s)**	**Cs (6s)**
LDFCP (relativistic)					
5.23	6.09	6.26	7.41	8.34	8.9
LDF (non-rel)					
length gauge					
5.1922	5.710	7.6332	8.6595	9.9185	10.650
velocity gauge					
5.1921	5.702	7.6332	8.6595	9.9185	10.650
local Kohn-Sham (non-rel)					
length gauge					
5.1312	5.673	7.6269	8.6596	9.9197	10.651
velocity gauge					
5.1307	5.669	7.6269	8.6595	9.9197	10.651
local CH (non-rel)					
length gauge					
5.1871	5.710	7.6453	8.672	9.9263	10.656
velocity gauge					
5.1871	5.710	7.6452	8.672	9.9263	10.656
5.17817[a]	5.75167[b]	7.770[c]			

[a]K. Pachucki, J. Komasa, PRL 68, 042507 (2003); [b]K. Pachucki, J. Komasa, PRL 92, 213001 (2004); [c]M. Lesiuk, J. Lang, PRA 108, 042817 (2023)

Conclusions

The LDFCP method:

- Allows one to obtain the energy spectrum and wave functions of an effective single-particle Hamiltonian.
- Provides a more accurate description of the fine structure and uses direct frequency integration in calculations of BBR shifts.
- Has low computational cost.
- Is not applicable for calculating the Bethe logarithm in the relativistic case.

The method gives results in reasonable agreement with the literature data for the considered atomic properties of alkali metals.

Bobylev, A., Solovyev, D., Zalialiutdinov, T. et al. Phys. Rev. A **113**(4), 042809 (2026).

Acknowledgments

Thank you for your attention!

This work is supported by the Foundation for the Advancement of Theoretical Physics and Mathematics “BASIS” (grant No. 25-1-2-18-4).

Appendix: core polarizabilities

Table 6: Values of the static core polarizability used in this work, in a.u.

Li	**Na**	**K**	**Rb**	**Cs**	**Fr**
0.192486	0.9947	5.354	9.1	15.81	20.4

J. Mitroy et al 2010 J. Phys. B: At. Mol. Opt. Phys. 43 202001

Appendix: scalar polarizability α_0 (cont.)

Table 7: Values of the static electric dipole scalar polarizability, α_0, in a.u. The data from Kiruga et al. (2026) are highlighted in blue

n	n^2S	$n^2P_{1/2}$	$n^2P_{3/2}$	$n^2D_{3/2}$	$n^2D_{5/2}$
			Li		
4	35336	262988	263020	4374090	4386700
	35281	273260	273230	4923700	4936000
			Na		
5	21539	-58981	-58387	4042970	4037220
	21697	-58620	-58027	4061600	4056700
			K		
5	4906	7027	7207	193843	192748
	4961	7023	7202	195000	194000
6	32470	43088	44326	712560	708266
	32840	43160	44390	718000	714000

n	n^2S	$n^2P_{1/2}$	$n^2P_{3/2}$	$n^2D_{3/2}$	$n^2D_{5/2}$
			Rb		
6	5127	12365	13361	92700	90345
	5167	12270	13270	94800	92400
7	32408	83363	90172	323139	313215
	32620	83150	90230	332900	322900
			Cs		
7	6162	31308	39256	-84121	-108868
	6232	29880	37510	-66600	-88800
			Fr		
8	4644	24118	45740	-36090	-91054
	4765	22670	43370	-19400	-73200

A. Kiruga et al, Computer Physics Communications 319, 109951 (2026)

Appendix: tensor polarizability α_2 (cont.)

Table 8: Values of the tensor electric dipole polarizability, α_2, in a.u. The data from Kiruga et al. (2026) are highlighted in blue.

n	$n^2P_{3/2}$	$n^2D_{3/2}$	$n^2D_{5/2}$
	Li		
4	-19644	-794916	-1138700
	-20708	-901800	-1291000
	Na		
5	2454	-925184	-1318620
	2488	-928210	-1323300
	K		
5	-1087	-37899	-53001
	-1063	-38200	-53400
	Rb		
6	-2079	28	4168
	-2060	-530	3490
	Cs		
7	-4588	79421	158795
	-4409	71040	141600
	Fr		
8	-6776	35254	157224
	-6599	31120	143100

A. Kiruga et al, Computer Physics Communications 319, 109951 (2026)

Appendix: BBR shifts (cont.)

Table 9: Values of the thermal (BBR) Stark shift at a temperature of 300 K, in Hz. The values from Farley and Wing (1981) are highlighted in blue.

n	n^2S	$n^2P_{1/2}$	$n^2P_{3/2}$	$n^2D_{3/2}$	$n^2D_{5/2}$
			Li		
4	-434.85	298.51	298.49	-224.59	-224.53
	-433.0	292.9		-219.2	
			Na		
5	-264.0	-259.5	-258.4	282.6	282.5
	-264.6	-254.8	-253.7	279.8	279.7
			K		
5	-45.378	-71.8	-73.87	379.7	379.7
	-45.76	-76.77	-78.97	357.3	358.7
6	-409.9	-447.23	-456.48	1389	1376
	-412.5	-427.1	-436.2	1293	1282

n	n^2S	$n^2P_{1/2}$	$n^2P_{3/2}$	$n^2D_{3/2}$	$n^2D_{5/2}$
			Rb		
6	-47.56	-142.9	-156.57	57.26	51.98
	-48.17	-151.8	-166.6	71.28	66.51
7	-409.7	-477.10	-466.86	575.7	538.2
	-411.7	-484.5	-473.8	593.8	554.2
			Cs		
7	-58.07	-147.4	-86.19	-797.7	-809.0
	-59.67	-153.4	-111.7	-810.4	-825.8
8	-470.1	412.7	406.9	-421.6	-306.2
	-477.4	410.6	425.2	-409.6	-299.4
			Fr		
8	-42.95	-230.6	-106.5	-641.0	-720.3
9	-319.7	198.8	360.0	-192.5	51.02

J. W. Farley, W. H. Wing, Phys. Rev. A 23, 2397 (1981)

Appendix: hyperfine structure

The hyperfine structure constant A of an $S_{1/2}$ state (the splitting between the levels $F = I \pm 1/2$ is $A(I + 1/2)$) is calculated by the following formula:

$$A = -\frac{\alpha^2}{m_p} \frac{\kappa g_I}{J(J+1)} \int_0^\infty dr\, g_a(r) \frac{1}{r^2} f_a(r). \tag{14}$$

Here α is the fine-structure constant, m_p is the proton mass (in atomic units), κ is the relativistic angular quantum number, J is the total angular momentum of the electron, $g_I = \mu/(\mu_N I)$ is the nuclear g-factor, where μ_N is the nuclear magneton.

Table 10: The hyperfine structure constant A in MHz (^{7}Li, ^{23}Na, ^{39}K, ^{87}Rb, ^{133}Cs).

	Li (2s)	**Na** (3s)	**K** (4s)	**Rb** (5s)	**Cs** (6s)
LDFCP	308.6 (23)	879.1 (0.7)	253.98 (10)	3627.12 (6)	2407.0 (5)
LDF	380.01 (5.4)	784.93 (11)	191.952 (17)	2892.73 (15)	1966.58 (14)
Exp.	401.7	885.8	230.8	3417.3	2298.1

E. Arimondo et al., Rev. Mod. Phys. **49**, 31 (1977)